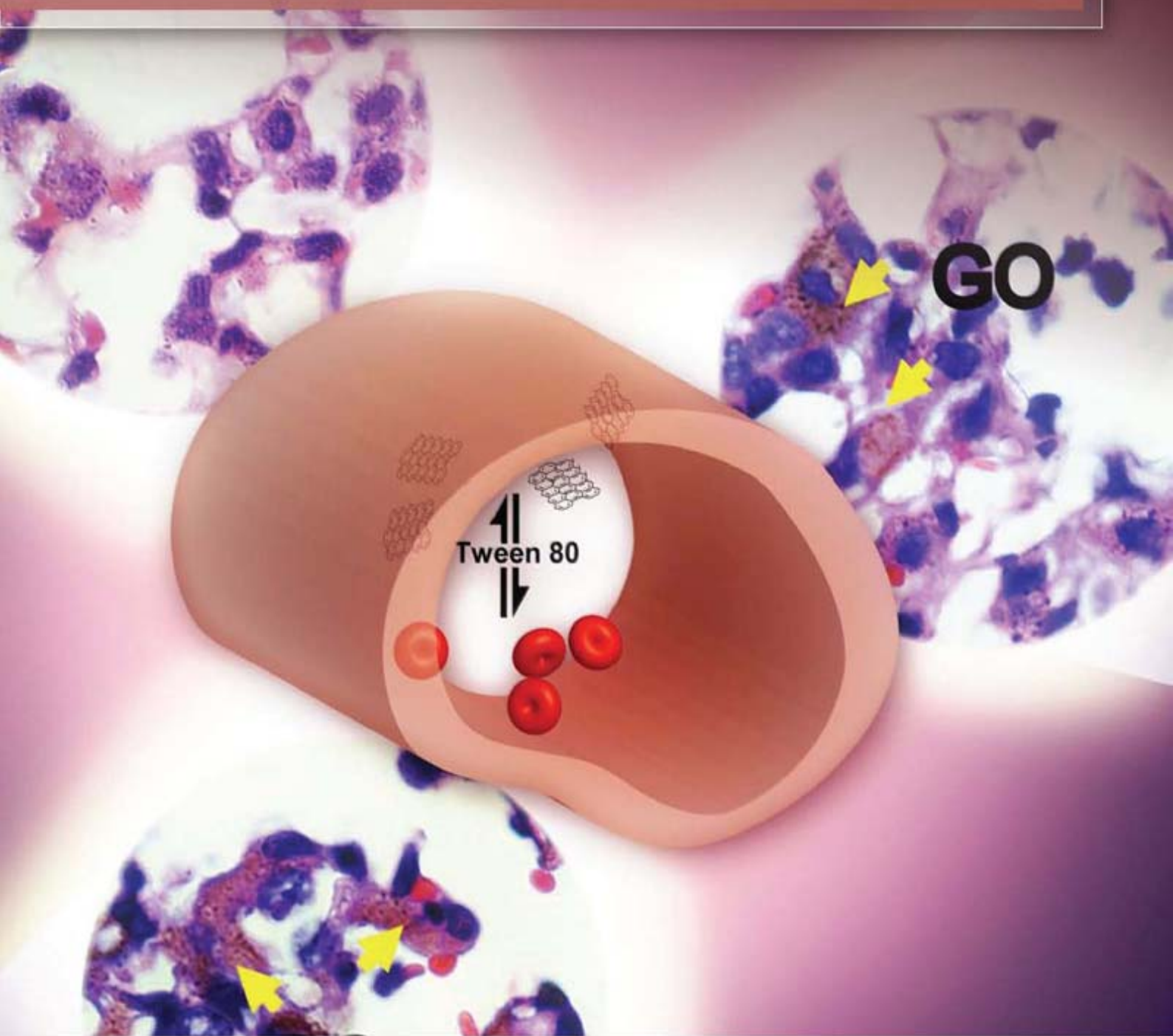


JES

JOURNAL OF
ENVIRONMENTAL
SCIENCES

ISSN 1001-0742
CN 11-2529/X

May 1, 2013 Volume 25 Number 5
www.jesc.ac.cn



Sponsored by
Research Center for Eco-Environmental Sciences
Chinese Academy of Sciences

CONTENTS

Environmental biology

Continuous live cell imaging of cellulose attachment by microbes under anaerobic and thermophilic conditions
using confocal microscopy

Zhi-Wu Wang, Seung-Hwan Lee, James G. Elkins, Yongchao Li, Scott Hamilton-Brehm, Jennifer L. Morrell-Falvey 849

Response of anaerobes to methyl fluoride, 2-bromoethanesulfonate and hydrogen during acetate degradation

Liping Hao, Fan Lü, Lei Li, Liming Shao, Pinjing He 857

Effect of airflow on biodrying of gardening wastes in reactors

F. J. Colomer-Mendoza, L. Herrera-Prats, F. Robles-Martínez, A. Gallardo-Izquierdo, A. B. Piña-Guzmán 865

Environmental health and toxicology

The *ex vivo* and *in vivo* biological performances of graphene oxide and the impact of surfactant on graphene
oxide's biocompatibility (Cover story)

Guangbo Qu, Xiaoyan Wang, Qian Liu, Rui Liu, Nuoya Yin, Juan Ma, Liquan Chen, Jiuyang He, Sijin Liu, Guibin Jiang 873

Determination of the mechanism of photoinduced toxicity of selected metal oxide nanoparticles (ZnO, CuO, Co₃O₄ and
TiO₂) to *E. coli* bacteria

Thabitha P. Dasari¹, Kavitha Pathakoti², Huey-Min Hwang 882

Joint effects of heavy metal binary mixtures on seed germination, root and shoot growth, bacterial bioluminescence,
and gene mutation

In Chul Kong 889

Atmospheric environment

An online monitoring system for atmospheric nitrous acid (HONO) based on stripping coil and ion chromatography

Peng Cheng, Yafang Cheng, Keding Lu, Hang Su, Qiang Yang, Yikan Zou, Yanran Zhao,

Huabing Dong, Limin Zeng, Yuanhang Zhang 895

Formaldehyde concentration and its influencing factors in residential homes after decoration at Hangzhou, China

Min Guo, Xiaoqiang Pei, Feifei Mo, Jianlei Liu, Xueyou Shen 908

Aquatic environment

Flocculating characteristic of activated sludge flocs: Interaction between Al³⁺ and extracellular polymeric substances

Xiaodong Ruan, Lin Li, Junxin Liu 916

Speciation of organic phosphorus in a sediment profile of Lake Taihu II. Molecular species and their depth attenuation

Shiming Ding, Di Xu, Xiuling Bai, Shuchun Yao, Chengxin Fan, Chaosheng Zhang 925

Adsorption of heavy metal ions from aqueous solution by carboxylated cellulose nanocrystals

Xiaolin Yu, Shengrui Tong, Maofa Ge, Lingyan Wu, Junchao Zuo, Changyan Cao, Weiguo Song 933

Synthesis of mesoporous Cu/Mg/Fe layered double hydroxide and its adsorption performance for arsenate in aqueous solutions

Yanwei Guo, Zhiliang Zhu, Yanling Qiu, Jianfu Zhao 944

Advanced regeneration and fixed-bed study of ammonium and potassium removal from anaerobic digested wastewater
by natural zeolite

Xuejun Guo, Larry Zeng, Xin Jin 954

Eutrophication development and its key regulating factors in a water-supply reservoir in North China	
Liping Wang, Lusan Liu, Binghui Zheng	962
Laboratory-scale column study for remediation of TCE-contaminated aquifers using three-section controlled-release potassium permanganate barriers	
Baoling Yuan, Fei Li, Yanmei Chen, Ming-Lai Fu	971
Influence of Chironomid Larvae on oxygen and nitrogen fluxes across the sediment-water interface (Lake Taihu, China)	
Jingge Shang, Lu Zhang, Chengjun Shi, Chengxin Fan	978
Comparison of different phosphate species adsorption by ferric and alum water treatment residuals	
Sijia Gao, Changhui Wang, Yuansheng Pei	986
Removal efficiency of fluoride by novel Mg-Cr-Cl layered double hydroxide by batch process from water	
Sandip Mandal, Swagatika Tripathy, Tapswani Padhi, Manoj Kumar Sahu, Raj Kishore Patel	993
Determining reference conditions for TN, TP, SD and Chl- <i>a</i> in eastern plain ecoregion lakes, China	
Shouliang Huo, Beidou Xi, Jing Su, Fengyu Zan, Qi Chen, Danfeng Ji, Chunzi Ma	1001
Nitrate in shallow groundwater in typical agricultural and forest ecosystems in China, 2004–2010	
Xinyu Zhang, Zhiwei Xu, Xiaomin Sun, Wenyi Dong, Deborah Ballantine	1007
Influential factors of formation kinetics of flocs produced by water treatment coagulants	
Chunde Wu, Lin Wang, Bing Hu, Jian Ye	1015
Environmental catalysis and materials	
Characterization and performance of Pt/SBA-15 for low-temperature SCR of NO by C ₃ H ₆	
Xinyong Liu, Zhi Jiang, Mingxia Chen, Jianwei Shi, Wenfeng Shangguan, Yasutake Teraoka	1023
Photo-catalytic decolourisation of toxic dye with N-doped titania: A case study with Acid Blue 25	
Dhruba Chakraborty, Susmita Sen Gupta	1034
Pb(II) removal from water using Fe-coated bamboo charcoal with the assistance of microwaves	
Zengsheng Zhang, Xuejiang Wang, Yin Wang, Siqing Xia, Ling Chen, Yalei Zhang, Jianfu Zhao	1044
Serial parameter: CN 11-2629/X*1989*m*205*en*P*24*2013-5	



Characterization and performance of Pt/SBA-15 for low-temperature SCR of NO by C₃H₆

Xinyong Liu¹, Zhi Jiang¹, Mingxia Chen¹, Jianwei Shi¹,
Wenfeng Shangguan^{1,*}, Yasutake Teraoka²

1. Research Center for Combustion and Environmental Technology, Shanghai Jiao Tong University, Shanghai 200240, China.

E-mail: liuxinyong520@hotmail.com

2. Department of Energy and Material Sciences, Faculty of Engineering Sciences, Kyushu University, Kasuga, Fukuoka 816-8580, Japan

Received 16 July 2012; revised 11 September 2012; accepted 14 September 2012

Abstract

Pt supported on mesoporous silica SBA-15 was investigated as a catalyst for low temperature selective catalytic reduction (SCR) of NO by C₃H₆ in the presence of excess oxygen. The prepared catalysts were characterized by means of XRD, BET surface area, TEM, NO-TPD, NO/C₃H₆-TPO, NH₃-TPD, XPS and ²⁷Al MAS NMR. The effects of Pt loading amount, O₂/C₃H₆ concentration, and incorporation of Al into SBA-15 have been studied. It was found that the removal efficiency increased significantly after Pt loading, but an optimal loading amount was observed. In particular, under an atmosphere of 150 ppm NO, 150 ppm C₃H₆, and 18 vol.% O₂, 0.5% Pt/SBA-15 showed remarkably high catalytic performance giving 80.1% NO_x reduction and 87.04% C₃H₆ conversion simultaneously at 140°C. The enhanced SCR activity of Pt/SBA-15 is associated with its outstanding oxidation activities of NO to NO₂ and C₃H₆ to CO₂ in low temperature range. The research results also suggested that higher concentration of O₂ and higher concentration of C₃H₆ favored NO removal. The incorporation of Al into SBA-15 improved catalytic performance, which could be ascribed to the enhancement of catalyst surface acidity caused by tetrahedrally coordinated AlO₄. Moreover, the catalysts could be easily reused and possessed good stability.

Key words: low-temperature; selective catalytic reduction; C₃H₆; Pt/SBA-15

DOI: 10.1016/S1001-0742(12)60107-7

Introduction

NO_x (NO+NO₂) exhausted from vehicles and stationary combustion engines is one of the important causes of photochemical smog, acid rain, and ozone depletion, which possess serious challenges to human health and environmental protection. With the increase of the motor vehicles, the problems caused by exhaust gas pollution are being much more serious. However, the traditional three-way catalysts (TWC) are not effective for the removal of low-concentration, oxygen-rich and low-temperature exhausts emitted from lean-burn engines and diesel vehicles. Besides, the low efficiency of TWC during the cold start engine also represents an important issue (Guo et al., 2006; Bera and Hegde, 2011; Granger and Parvulescu, 2011). Therefore, it is of great significance to develop new catalysts with high performance for the treatment of low-concentration exhaust at low temperature.

Selective catalytic reduction (SCR) technique has been

proven to be one of the most effective methods for reducing NO_x emissions due to its high efficiency and simplicity (Liu and Woo, 2006; Roy et al., 2009). It is well known that NH₃-SCR is a widely practiced NO_x control technology (Brandenberger et al., 2008), but problems such as storage, transportation, leakage, corrosion of NH₃ and catalysts toxicity (vanadium species) are inevitable. Also, hydrocarbons (HCs) are a natural component already present in combustion exhaust, thus it is quite convenient and competitive to use HCs as reducing agent (HC-SCR). Usually, SCR technology requires rather higher reaction temperature (above 300°C), but if SCR of low concentration NO_x by HC occurs over catalyst with high deNO_x activity at low temperature, this technology could compete with NH₃-SCR and be more practical for the removal of NO_x in places such as urban road tunnels and underground parking lots.

Low temperature HC-SCR has been extensively studied and a large number of catalysts have been evaluated. Noble metal doped catalysts, e.g., Pt/Al₂O₃ (Salem et al., 2008;

* Corresponding author. E-mail: shangguan@sjtu.edu.cn

Seker and Gulari, 2002), Rh/TiO₂ (Halkides et al., 2002), Pt/V/MCM-41 (Jeon et al., 2003), Pt-Sn/Al₂O₃ (Corro et al., 2003), are promising due to the high activity at low temperatures and high SO₂ tolerance as well as good water resistance. In our recent work, 0.5% Pt/TiO₂ (anatase) was found to be the most active catalyst among a series of Pt supported TiO₂ catalysts for the low temperature C₃H₆-SCR in excess oxygen. Under the condition of 150 ppm NO, 150 ppm C₃H₆, and 18 vol.% O₂, this 0.5% Pt/TiO₂ catalyst could achieve a complete C₃H₆ conversion and 47.03% NO_x reduction simultaneously at 180°C (Liu et al., 2011). This indicates again that Pt loaded catalyst is promising for low temperature C₃H₆-SCR process.

Mesoporous molecular sieves have been recognized as the good catalytic supports for their high specific surface area, porous volume and adjustable pore size diameter as well as the uniform pore size distribution (Beck et al., 1992). Within the family of mesoporous materials, SBA-15 materials synthesized under acidic conditions exhibit larger pore size and thicker pore volume wall compared with M41S (Zhao et al., 1998). Its remarkably high surface area and large pore volume favoring a high dispersion of the active component on the surface of the catalytic support as well as the improved accessibility of active sites should have a favorable impact on catalytic activity (Sayari, 1996; Corma, 1997). Such mesoporous silica SBA-15 based catalysts were already studied in SCR of NO by ammonia (Rico et al., 2010; Segura et al., 2005; Chmielarz et al., 2006), CO (Patel et al., 2011) and by ethanol (Boutros et al., 2009), and exhibited various reduction activities toward NO_x at higher temperature (> 300°C). However, this pure siliceous mesoporous material is lack of acid sites and acidity, incorporation of Al into the structure of SBA-15 is an effective way to enhance its acidity which may promotes the SCR reactions (Giroir-Fendler et al., 2001; Brandhorst et al., 2005).

In the present work, we reported a Pt/SBA-15 catalyst that exhibited high activity for low temperature C₃H₆-SCR in the presence of excess O₂. Special emphasis is given to the possible correlations among Pt loading amount, O₂/C₃H₆ concentration, Al incorporation, and NO conversion efficiency of the catalysts. For practical consideration, catalytic stability of the prepared catalysts was investigated as well.

1 Experimental

1.1 Catalyst preparation

SBA-15 materials were synthesized according to the procedure reported in other literature (Zhao et al., 1998). In a typical synthesis, 4 g of the P123 (EO₂₀-PO₇₀-EO₂₀, Aldrich) was dissolved in 30 g of H₂O and 120 g of 2 mol/L HCl. The mixture was continually stirred for a few hours until the copolymer was completely dissolved. Then 8.5 g of tetraethylorthosilicate (TEOS) was slowly added

dropwise and the resulting mixture was stirred for 20 hr at 40°C. Afterward, the samples were aged at 100°C in the autoclave for 24 hr. After cooling, the solids were washed and filtered with deionized water, and then allowed to air-dry. Finally, the as-synthesized samples were calcined at 550°C for 6 hr in air to obtain mesoporous SBA-15.

In a typical Al-SBA-15 synthesis (Yue et al., 1999): 8.5 g TEOS and a calculated amount isopropoxide aluminium, to obtain a given Si/Al ratio (10), were added to 10 mL of aqueous HCl at pH 1.5. This mixture was stirred for 4 hr at room temperature and then added to a second solution containing 4 g of P123 in 150 g of aqueous HCl at pH 1.5. The resulting solution was stirred for 20 hr at 40°C, followed by aging at 100°C for 24 hr under static conditions. The solid product was recovered by filtration, dried at room temperature and calcined at 550°C for 6 hr. The as-synthesized sample was denoted as Al-SBA-15(10), where 10 is the Si/Al ratio.

All Pt supported catalysts were prepared by impregnating weighted supports with calculated amounts of Pt(NH₃)₂(NO₂)₂ aqueous solution, followed by 30 min of ultrasonic dispersion. Then all catalysts were dried at 110°C for 12 hr followed by calcination in air at 450°C for 4 hr. All the above catalysts were ground and sieved to 40–60 mesh for evaluation.

1.2 Characterization of catalysts

The powder X-ray diffraction (XRD) measurements were carried out with a Rigaku D/max-2200/PC X-ray diffractometer (Rigaku Corporation, Japan) with Cu K α radiation and operated at 49 kV and 20 mA.

Measurements of the BET surface area were performed by nitrogen adsorption data from Quantachrome NO-VA1000a Sorptomatic apparatus (Quantachrome, USA).

Transmission electron microscopic (TEM) images were obtained by employing a JEM-2010 (JEOL, Japan) device with a 200-kV accelerating voltage.

X-ray photoelectron spectroscopy (XPS) spectra were acquired with a Kratos Axis Ultra^{DLD} spectrometer (Shimadzu-Kratos, Japan) using a monochromatic Al K α source (1486.6 eV). The BE scale was calibrated according to the C1s peak (284.8 eV) for adventitious carbon on the analyzed sample surface.

²⁷Al MAS NMR experiment was performed at room temperature with a 4.0 mm MAS probe on a Bruker Avance III-400 spectrometer (Bruker, Swiss) in a magnetic field strength of 9.4 T at a frequency of 104.263 MHz. Powder sample was packed inside zirconia MAS rotors and spun at 10 kHz. A single pulse 2.0 μ s followed by acquisition of 1 K points was repeated at a recycle rate of 3 sec.

1.3 Catalytic activity test

Catalytic activity of the catalysts for NO reduction was determined in a continuous fixed bed U-type quartz reactor (Shanghai Zhiying, China) (4 mm i.d.) using 0.2 g of

catalyst. The standard reactant composition was as follows: 150 ppm C₃H₆, 150 ppm NO, 18 vol.% O₂, and Ar balance at a total flow rate of 120 mL/min. The concentrations of NO, NO₂ and NO_x were monitored by a chemiluminescent NO/NO₂ analyzer (Thermo Environmental Instruments Inc., 42i LS, Thermo, USA). C₃H₆ and CO₂ were determined by a gas chromatograph (GC, Shanghai Huaai, China) equipped with a flame ionization detector (FID) detector, and a quadrupole mass spectrometer (Ametek Process Instruments, Dycor DM 100M, USA) was also used combined with a GC. The data were collected when the reactions reached the steady state around 40 min at each temperature point. Unless otherwise specified, the gas flow rates in this article were all fixed at 120 mL/min. The NO_x removal efficiency (R , %) was calculated as follows:

$$R = \frac{[\text{NO}_x]_{\text{in}} - [\text{NO}_x]_{\text{out}}}{[\text{NO}_x]_{\text{in}}} \times 100\% \quad (1)$$

where, $[\text{NO}_x]_{\text{in}}$ is the inlet concentration of NO_x and $[\text{NO}_x]_{\text{out}}$ is the outlet concentration of NO_x.

1.4 NO temperature programmed desorption

Before the TPD experiment, the samples were pretreated in pure Ar flow at 350°C for 30 min then cooled down to 50°C. Adsorption of NO was carried out over 0.2 g catalyst by passing a flow of 150 ppm NO and 18 vol.% O₂ balanced with Ar through the sample bed at 50°C for 1 hr. After the sample was purged with Ar for 20 min at 50°C, the TPD experiment was performed with a heating rate 4°C/min.

1.5 Oxidation of NO and oxidation of C₃H₆

Oxidation of NO/C₃H₆ was also carried out with a heating rate 4°C/min. The feed gas mixture was 150 ppm NO/150 ppm C₃H₆ and 18 vol.% O₂ balanced with Ar, 0.2 g catalyst was used as well.

1.6 NH₃ temperature programmed desorption

The surface acidity of the samples was determined by a temperature programmed desorption of ammonia (NH₃-TPD) in a fixed-bed quartz reactor. The 0.2 g catalyst sample was first pretreated in pure N₂ at 500°C for 1 hr to yield a clear surface, and was then cooled down to 50°C. The cooled sample was exposed and saturated with 600 ppm NH₃/N₂ at a flow rate of 150 mL/min for 1–2 hr, and was then purged by N₂ until constant baseline level was attained. In the desorption process, the carried gas N₂ was kept at a flow rate of 150 mL/min while the temperature was raised from 50 to 500°C with a heating rate of 5°C/min. The effluent composition was analyzed continuously with a FT-IR spectrometer (Thermo Nicolet 6700, USA).

2 Results and discussion

2.1 Catalysts characterization

Small-angle and wide-angle X-ray diffraction patterns of the synthesized catalysts are presented in **Fig. 1**. As can be seen from **Fig. 1a**, both samples exhibited well resolved diffraction peaks that can be indexed as the (100), (110) and (200) reflections associated with *P6mm* hexagonal symmetry typical of SBA-15 materials (Zhao et al., 1998). Comparing two samples, the diffraction peaks of Al-SBA-15(10) were slightly shifted to lower values than those of SBA-15. This fact is related with the longer Al–O bond length compared to the Si–O bond (Calleja et al., 2007).

Figure 1b illustrates the wide-angle XRD patterns of the synthesized catalysts. All materials exhibited a broad diffraction peak between 15°–35°, corresponding to the amorphous silica. No diffraction peak of alumina was found on the wide-angle XRD pattern of Al-SBA-15(10), meaning the well dispersion of alumina and no formation of Al₂O₃ crystallites in this sample. Additionally, the XRD pattern of Pt supported catalysts also showed weak reflection peaks at about 39.7°, 46.2° and 67.5°, attributed

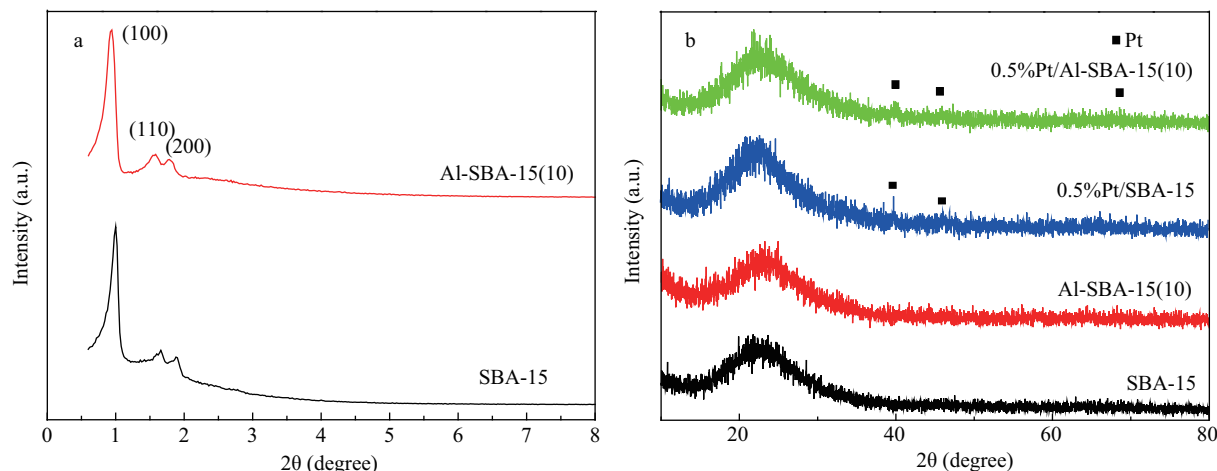


Fig. 1 XRD-patterns of synthesized catalysts. (a) small angle XRD; (b) wide angle XRD.

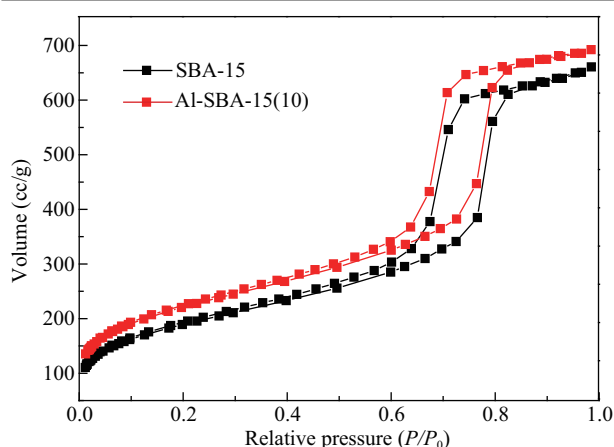


Fig. 2 Nitrogen adsorption-desorption isotherms of SBA-15 and Al-SBA-15(10).

to the metallic state platinum.

The nitrogen adsorption-desorption isotherms of SBA-15 and Al-SBA-15 materials are depicted in **Fig. 2**. It is obvious that both isotherms are Type IV (IUPAC classification) with H1 hysteresis loops at high relative pressure values (Ravikovitch and Neimark, 2001; Jang et al., 2004), corresponding to the mesoporous materials consisting of well-defined cylindrical-like pore channels and a high degree of pore size uniformity, which can also be observed in **Fig. 3**. BET surface areas were calculated from physisorption data of the samples. **Table 1** gives the textural properties of the Al-SBA-15(10) sample, together with the data of SBA-15 for comparison.

Representative TEM images of the synthesized catalysts are displayed in **Fig. 3**. **Figure 3a** and **c** show representative images along the [100] direction of SBA-15 and [001] direction of Al-SBA-15(10), respectively. The high degree of order and the characteristic hexagonal features of SBA-15 are maintained in Al-SBA-15(10) after aluminium incorporation, which is in good agreement with the small-angle XRD results above. **Figure 3b** and **d** reveal the long ordered arrangement of the channels in SBA-15 and Al-SBA-15(10) on which platinum nanoparticles are uniformly distributed, indicating that the ordered frameworks were retained after the impregnation process. These particles are present in a good distribution of size smaller than 8.0 nm.

Figure 4 shows the XPS spectra of Pt 4f region on Pt/SBA-15 with the fitting result presented in the table. For the sample, metallic Pt⁰ (binding energy at 71.2 and 74.6 eV), Pt^{II}O (binding energy at 72.3 and 75.6 eV) (Pitchon and Fritz, 1999) and Pt^{IV}O₂ (binding energy at 74.3 and

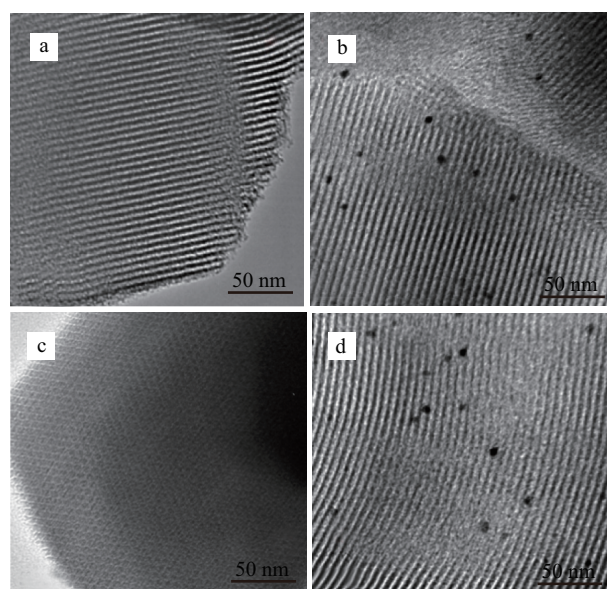


Fig. 3 TEM images of synthesized catalysts. (a) SBA-15; (b) 0.5% Pt/SBA-15; (c) Al-SBA-15(10); (d) 0.5% Pt/Al-SBA-15(10).

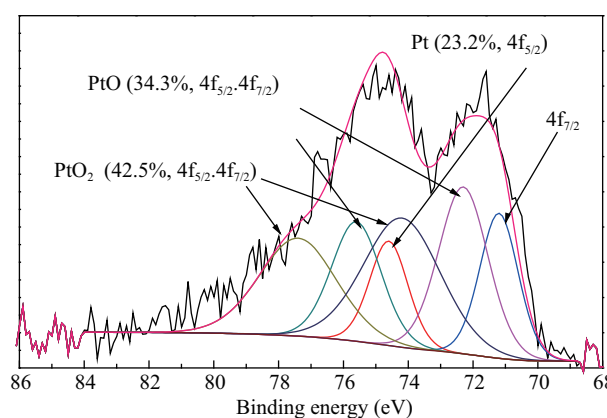


Fig. 4 Pt 4f XPS spectra of Pt/SBA-15.

77.8 eV) (Li et al., 2011) were all observed on SBA-15 support. In particular, the relative peak areas of PtO₂ were somewhat larger compared with the other Pt species. This suggests that the PtO₂ species might play a role as an active site in deNO_x. In the meantime, the analysis of Pt 4d region was utilized to detect Pt species supported on Al-SBA-15. For the aluminosilica sample, Pt (314.4 eV), PtO (314.9 eV) and PtO₂ (317.9 eV) (www.lasurface.com) were also observed on the support, however, the fitting result was not so accurate as Pt/SBA-15 sample.

2.2 Catalytic activity tests

A comparative study of NO catalytic reduction by C₃H₆ in the presence of 18% O₂ was carried out over SBA-15 and 0.5% Pt/SBA-15. The 0.5% Pt/SBA-15 achieved 80.1% NO reduction (**Fig. 5a**) and 87.04% C₃H₆ conversion to CO₂ (**Fig. 5b**) simultaneously at 140°C, which were significantly higher than those of SBA-15. As shown in **Fig. 5a**, with the temperature increasing from 100 to 340°C, the NO_x reduction efficiency of the catalysts increased until

Table 1 Physicochemical properties of synthesized catalysts

Sample	Al _{tetra} /Al _{octa}	S _{BET} (m ² /g)	Pore size (nm)	Pore volume (cm ³ /g)
SBA-15	—	645.4	6.295	1.016
Al-SBA-15(10)	1.67	737.5	7.12	1.160

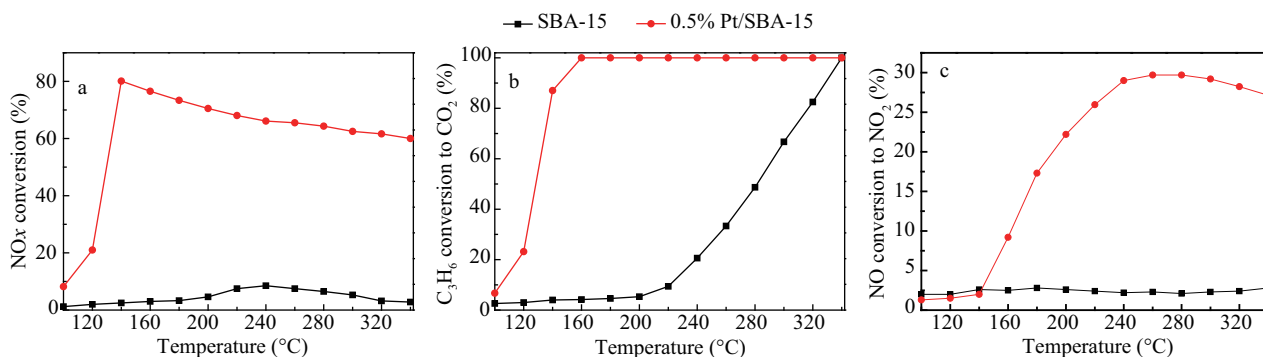


Fig. 5 Catalytic activity as a function of reaction temperatures in C₃H₆-SCR process over SBA-15 and 0.5% Pt/SBA-15. (a) NO_x conversion; (b) C₃H₆ conversion to CO₂; (c) NO conversion to NO₂. Reaction conditions: [NO] = [C₃H₆] = 150 ppm, [O₂] = 18%, balance Ar, total flow rate 120 mL/min.

reached the maximum, and then decreased. The lowering NO_x reduction efficiency at high temperature range could be ascribed to competitive reactions of C₃H₆ oxidation involving in SCR and direct C₃H₆ combustion. In other words, C₃H₆ were more readily oxidized by O₂ other than to form C_xH_yO_z at high temperature, which was supposed to be critical intermediate in HC-SCR reaction. As shown in **Fig. 5b**, the C₃H₆ conversion to CO₂ increased with temperature increasing before reaching the 100% platform. Additionally, only CO₂ was detected as the product of C₃H₆ oxidation during SCR reaction of SBA-15 support and Pt/SBA-15 catalyst, which indicates that the catalyst and support have 100% selectivity towards CO₂.

2.3 NO temperature programmed desorption

Figure 6 shows the TPD profiles corresponding to the NO concentration. It is obvious that Pt loading favored the adsorption of NO, namely, the desorption amount is six times higher in Pt/SBA-15 than in SBA-15 (Pt/SBA-15: 25.18 μmol/g; SBA-15: 4.01 μmol/g), which could be explained by Pt–NO species formation mechanism (Kotsifa et al., 2007; Ivanova et al., 2007).

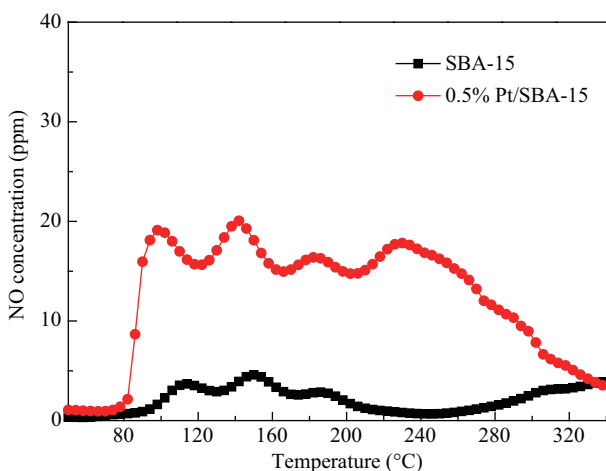


Fig. 6 NO-TPD profiles of SBA-15 and 0.5% Pt/SBA-15.

2.4 Oxidation of NO and oxidation of C₃H₆

Oxidation activities of NO to NO₂ by O₂ on SBA-15 and Pt/SBA-15 were investigated and compared in **Fig. 7a**. SBA-15 had very poor oxidizing ability in the whole temperature range, while the oxidative activity on Pt/SBA-15 increased rapidly with temperature increasing, and then kept a high level followed by a little decrease at elevated temperatures (above 280 °C), this decrease could be ascribed to the thermodynamic equilibrium, i.e., NO₂ ↔ NO + 1/2O₂. The Pt/SBA-15 showed absolutely higher oxidation activity in the whole temperature range than SBA-15 and even Pt/TiO₂ (Liu et al., 2011). This is in good accordance with the catalytic performance obtained in SCR reaction (**Fig. 5**). Some researchers even found that the conversion of NO_x was significantly improved by replacing the feed reaction gas NO with NO₂ directly (Li et al., 2004; Liu and Woo, 2006). The as-formed NO₂ is easily to form nitrates (nitrites) over the catalyst surface, which were regarded as important intermediates of SCR reaction. It was generally accepted that the nitrates derived from NO₂ can be readily reduced to N₂ by oxygenated species originated from HCs on the catalyst surface subsequently (García-Cortés et al., 2000; Matyshak et al., 2009; Nguyen et al., 2010). Compared the NO₂ formation in NO oxidation reaction (**Fig. 7a**) with SCR reaction (**Fig. 5c**), it is found that NO₂ formation was somewhat inhibited by the introduction of C₃H₆, as also reported in other literature (Yentekakis et al., 2005).

C₃H₆ oxidation activities of SBA-15 and Pt/SBA-15 are plotted in **Fig. 7b**. SBA-15 could oxidize C₃H₆ (*m/e* = 41 signal) completely at about 285 °C, whereas Pt/SBA-15 oxidized C₃H₆ completely to CO₂ at much lower temperature, say, at around 115 °C, indicating that Pt loading favors the C₃H₆ oxidation. By the way, this temperature is about 20 °C lower than that of Pt/TiO₂ (Liu et al., 2011). C₃H₆ is activated on the surface of the noble metal loaded catalyst by forming oxygenated species (C_xH_yO_z) with the participation of oxygen (Gorce et al., 2004; Adamowska et al., 2009); and an efficient catalyst should preferentially promote oxidation of adsorbed C₃H₆ with Pt–O (Kotsifa

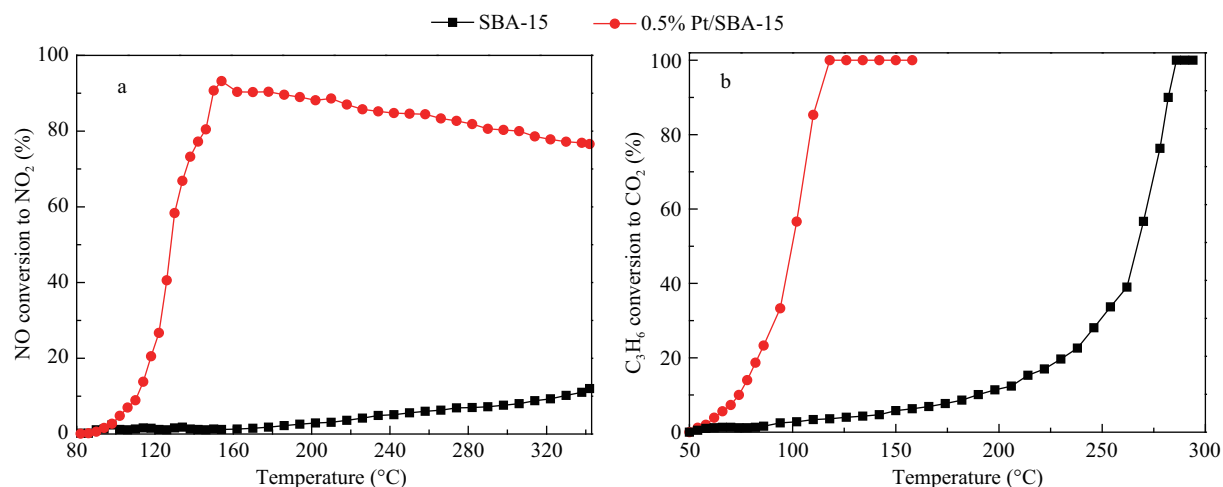


Fig. 7 NO oxidation (a) and C₃H₆ oxidation (b) profiles of SBA-15 and 0.5% Pt/SBA-15.

et al., 2007). Comparing Fig. 7b and Fig. 5b, it could be observed that the presence of NO in the C₃H₆-SCR reaction increased the C₃H₆ light-off temperature and the temperature of 100% C₃H₆ conversion by 50–60°C; the C₃H₆ oxidation was also somewhat inhibited by NO participation in SCR. It is presumed that the inhibition of C₃H₆ oxidation induced by NO and that of NO₂ formation caused by C₃H₆ at low temperatures are due to the competition of reaction intermediates for active surface sites (Yentekakis et al., 2005). Concerning the results obtained in the catalytic activity tests (Section 2.2), it could be concluded that the remarkable low temperature C₃H₆-SCR performance was correlative well with the enhanced oxidation activities of NO to NO₂ and C₃H₆ to CO₂ at low temperature.

2.5 Factors influencing NO conversion

2.5.1 Effect of O₂ concentration

The effect of O₂ concentration on the C₃H₆-SCR activity of the 0.5% Pt/SBA-15 catalyst was examined. The oxygen concentration increased from 6% to 18%, while its

effect on NO_x reduction and C₃H₆ conversion over this catalyst is plotted in Fig. 8. Higher O₂ concentration in the feed increased the maximum NO_x reduction activity from 77.6% (6% O₂) to 78.37% (12% O₂) and finally to 80.1% (18% O₂). At the same time, the T_{\max} (temperature for maximum NO_x conversion) lowered from 180°C to 160°C and 140°C, respectively. The conversion of C₃H₆ was also shifted toward the low temperature range with the increase of oxygen concentration. The positive effect of excess O₂ is also reported in other literature (Haneda et al., 2003; Yentekakis et al., 2005; Li et al., 2004). These results indicate that oxygen plays a key role in C₃H₆-SCR, and could be explained as follows (Li et al., 2004; Iliopoulou et al., 2004; Wang et al., 2005). Oxygen would contribute to several reaction steps such as hydrocarbon partially oxidized forming intermediate active species C_xH_yO_z, reacting with NO_x (NO, NO(a) + O(a) → NO₂), which leads to NO_x removal. Increasing the O₂ concentration enhances the formation of intermediate active species of hydrocarbons and the activation of NO, thus increasing NO_x reduction.

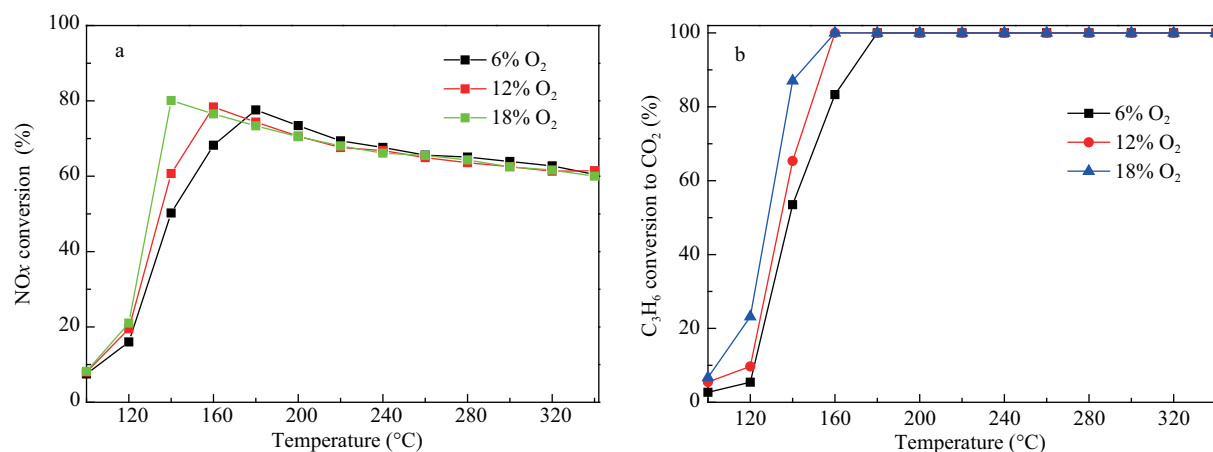


Fig. 8 Effect of O₂ concentration on NO_x conversion and C₃H₆ conversion over 0.5% Pt/SBA-15 catalyst. Reaction conditions: [NO] = [C₃H₆] = 150 ppm, balance Ar, total flow rate 120 mL/min.

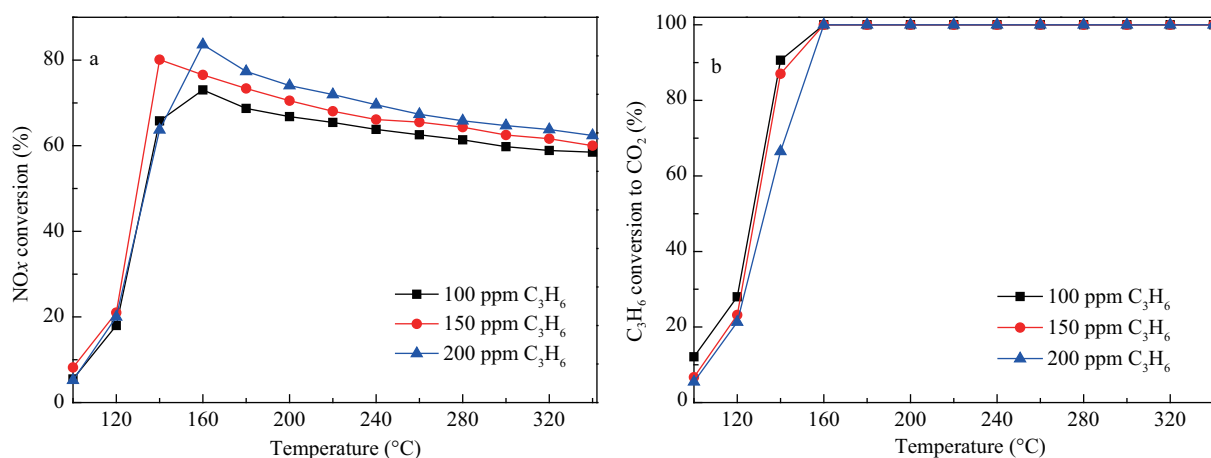


Fig. 9 Effect of C₃H₆ concentration on NO_x conversion and C₃H₆ conversion over 0.5% Pt/SBA-15 catalyst. Reaction conditions: [NO] = 150 ppm, [O₂] = 18%, balance Ar, total flow rate 120 mL/min.

2.5.2 Effect of C₃H₆ concentration

The effect of C₃H₆ concentration on NO_x reduction over 0.5% Pt/SBA-15 was evaluated and compared. As shown in **Fig. 9a**, with the increase of C₃H₆ concentration, the maximum NO_x reduction activity increased from 73.02% (100 ppm C₃H₆) to 80.1% (150 ppm C₃H₆) and finally to 83.6% (200 ppm C₃H₆). However, the T_{\max} varied from 140°C (150 ppm C₃H₆) to 160°C (100 ppm C₃H₆; 200 ppm C₃H₆). In the meantime, the conversion of C₃H₆ shifted toward high temperature range as well. The result indicates that higher concentration of reductant is beneficial to the reduction of NO_x, which is in good agreement with previous reports (Jen, 1998; Lanza et al., 2009). Increasing C₃H₆ concentration enhances the formation of C_xH_yO_z, which is well regarded as a crucial intermediate active species in NO_x removal by HC-SCR, thereby facilitating NO reduction.

2.5.3 Effect of Pt loading

In **Fig. 10a**, the catalytic activities of NO_x reduction over SBA-15 with various Pt loading contents are shown as

a function of reaction temperature. Among all samples, 0.5% Pt/SBA-15 performed the most efficiently giving 80.1% NO_x reduction and 87.04% C₃H₆ conversion simultaneously at 140°C. In contrast, 0.2% Pt/SBA-15 reached maximum NO_x conversion efficiency of 33.3% and 100% C₃H₆ conversion at 180°C. Further increasing Pt content in the catalysts from 0.5% to 2% led to a decrease of maximum NO_x reduction activity from 80.1% (0.5% Pt) to 76.56% (1% Pt) and finally to 73.2% (2% Pt), but the T_{\max} was not changed. However, as shown in **Fig. 10b**, the C₃H₆ conversions increased monotonously with reaction temperature increasing, and the temperatures at which C₃H₆ was completely consumed were decreased on higher Pt loading samples.

Considering the correlations between Pt loading amount and NO_x removal efficiency, the intermediate Pt loading of 0.5% is the optimum amount for NO_x reduction, which is similar to previous studies (Hoost et al., 1997; Luo et al., 2004; Iliopoulou et al., 2004). The Pt species (Pt, PtO_x) over catalyst surface are regarded as vital active sites for catalytic reactions. The number of active sites available

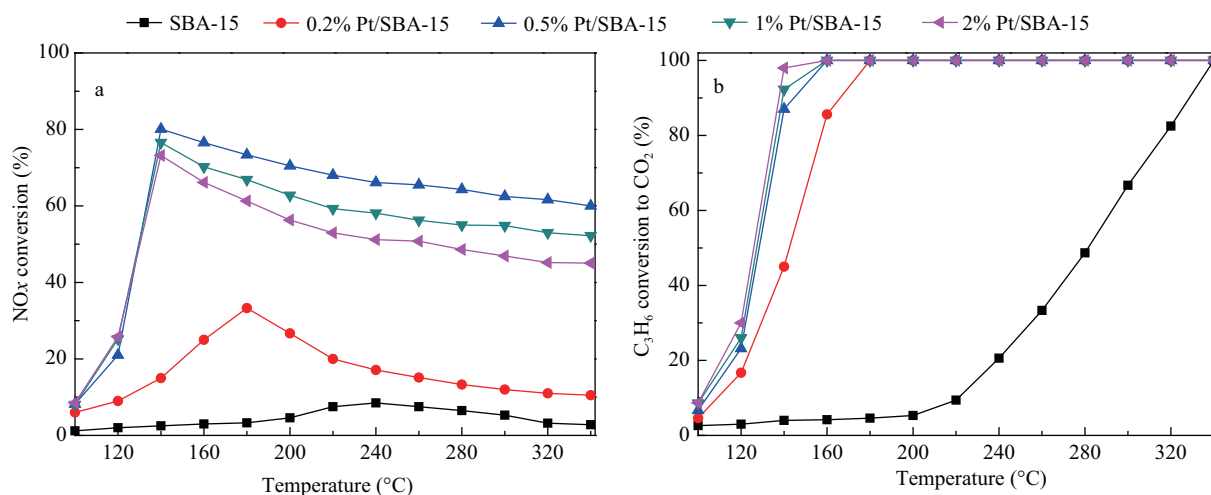


Fig. 10 NO_x conversion and C₃H₆ oxidation over Pt/SBA-15 with various Pt loadings. Reaction conditions: [NO] = [C₃H₆] = 150 ppm, [O₂] = 18%, balance Ar, total flow rate 120 mL/min.

for NO_x reduction increased with the increase of the Pt loading, but there was an optimum Pt loading amount (0.5% Pt), at which the number of active sites just meet the needs of NO_x SCR reaction. In other words, the Pt content of 0.5% was enough to activate the SCR reaction, while weakening the direct combustion of C₃H₆ with O₂. In case of 1% Pt and 2% Pt supported SBA-15, higher amount Pt would lead to a fortified direct combustion of C₃H₆, resulting in decreasing the amount of reductant remaining for the SCR reaction, which may in part explain their lower catalytic activities (Iliopoulou et al., 2004; Kumar et al., 2008).

2.5.4 Effect of Al incorporation

Al-SBA-15 was prepared by direct hydrothermal synthesis where isopropoxide aluminium used as Al source. The ²⁷Al MAS NMR spectrum of the Al-SBA-15 sample is displayed in Fig. 11. There were two resolved peaks in the spectrum at approx. 53 and 0 ppm, respectively. The former, which is attributable to tetrahedrally coordinated aluminum species, indicates that aluminum atoms have been incorporated into the framework of the siliceous samples (AlO₄ structural unit, Al(tet), and the aluminum is covalently bonded to four Si atoms by oxygen bridges). The resonance at 0 ppm can be assigned to octahedral

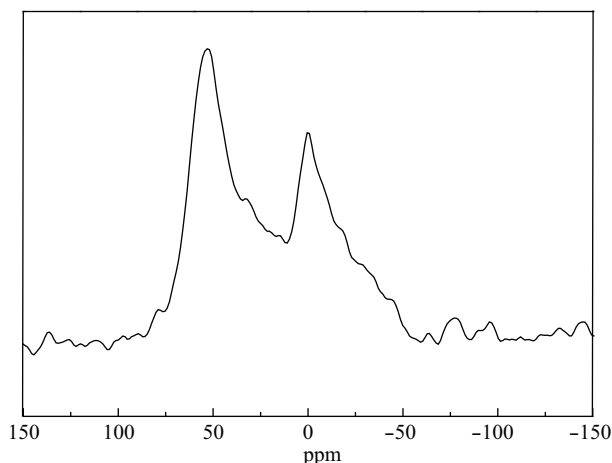


Fig. 11 Solid ²⁷Al MAS NMR spectrum of Al-SBA-15(10).

aluminum corresponding to extra-framework aluminum species (AlO₆ structure unit, Al(oct)) (Sumiya et al., 2001). Also, a small shoulder peak at around 30 ppm could be attributed to pentahedrally coordinated aluminum species (Al(penta)) (Yue et al., 1999). From the results of ²⁷Al MAS NMR spectrum and according to the peak area ratio of the tetrahedrally coordinated Al to octahedrally Al (Area 50 ppm/Area 0 ppm=1.67, Table 1), it can be proved that most of aluminum had been incorporated into the framework of SBA-15 sample.

Figure 12 shows that the catalytic activity for C₃H₆-SCR over Pt/SBA-15 was improved by the Al incorporation. The 0.5% Pt/Al-SBA-15(10) catalyst exhibited remarkably high activity in low temperature C₃H₆-SCR process, giving 86.06% NO_x reduction efficiency at T_{max} of 140°C. Improvement of the activity could be reasoned by the enhancement of surface acidity after Al incorporation which was evidenced by NH₃-TPD. As shown in Fig. 13, the TPD profile of Pt/SBA-15 material showed no evident peaks, indicating that Pt/SBA-15 material has no acid sites. In the meantime, the TPD profile of Pt/Al-SBA-15(10) material showed a main peak at about 120°C and a shoulder peak at around 200°C related to weak and mild acid sites, respectively, whereas the desorption peak of NH₃ is too broadened to be detected at a temperature higher than 300°C corresponding to strong acid sites. NH₃-TPD plots show that there is a substantial increase in acidity and acid strength after Al incorporation. Based on the NMR analysis results, NH₃-TPD profiles and other literature (Li et al., 2004), we can propose that the tetrahedrally coordinated AlO₄ contributes to the acidity greatly.

2.6 Stability of the catalysts

To evaluate the stability of the catalysts, the recycling experiments were performed for eight successive cycles under standard reaction condition in the temperature range between 100 and 340°C. It can be seen from Fig. 14 that the maximum NO_x conversion of both samples hardly decreased by and large after the fifth cycle even after the sixth cycle, whereas the T_{max} did not increase to 160°C until the sixth cycle. This indicated that the catalytic

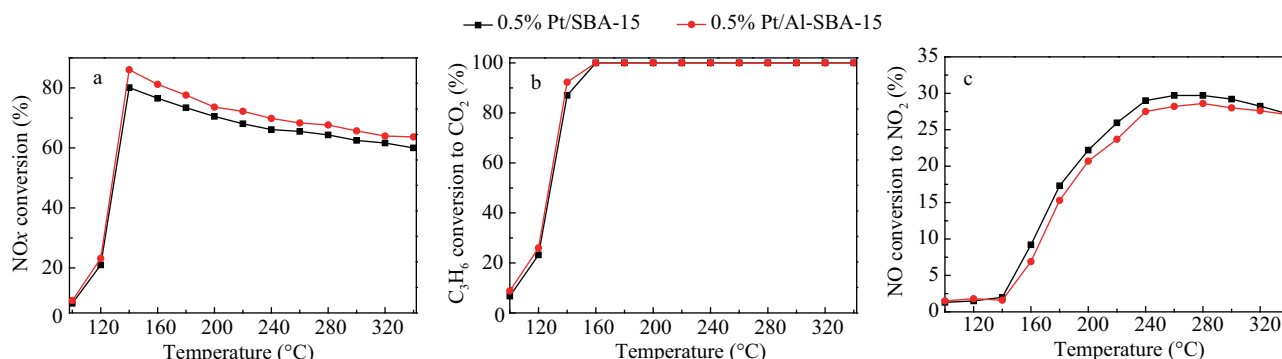


Fig. 12 Conversion of NO_x with the function of temperature over 0.5% Pt/SBA-15 and 0.5% Pt/Al-SBA-15. (a) NO_x conversion; (b) C₃H₆ conversion to CO₂; (c) NO conversion to NO₂. Reaction conditions: [NO] = [C₃H₆] = 150 ppm, [O₂] = 18%, balance Ar, total flow rate 120 mL/min.

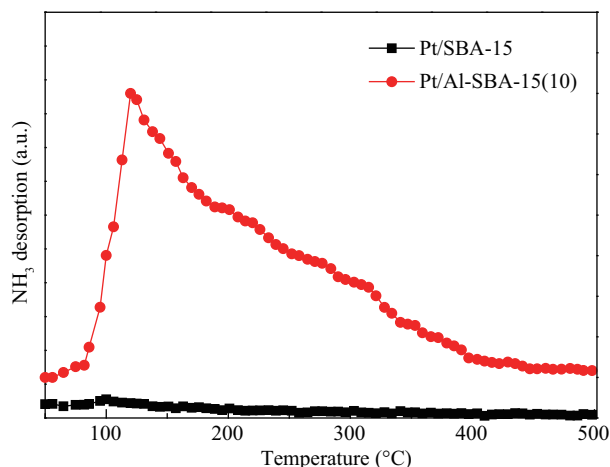


Fig. 13 NH₃-TPD profiles of Pt/SBA-15 and Pt/Al-SBA-15(10)

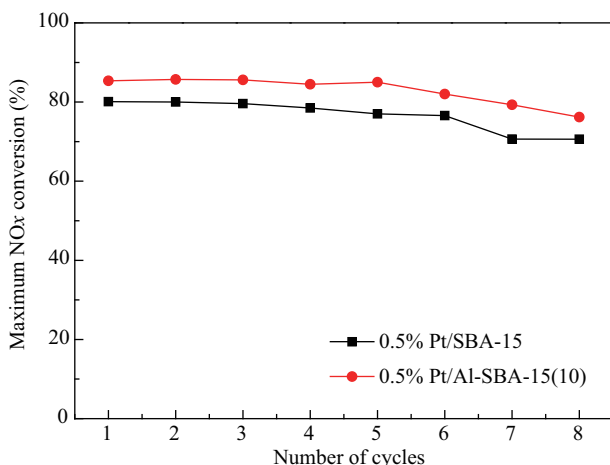


Fig. 14 Recycling investigations of 0.5% Pt/SBA-15 and 0.5% Pt/Al-SBA-15(10) in SCR reaction. T_{\max} of the cycle 1–5 was 140°C, and T_{\max} of the cycle 6–8 was 160°C. Reaction conditions: [NO] = [C₃H₆] = 150 ppm, [O₂] = 18%, balance Ar, total flow rate 120 mL/min.

performance of both catalysts is well-sustained. However, obvious deactivation was observed after the seventh and the eighth cycle for both catalysts, say, the maximum NO_x conversion efficiency of the eighth cycle were 70.6% for 0.5% Pt/SBA-15 and 76.2% for 0.5% Pt/Al-SBA-15(10) respectively. In addition, the T_{\max} of these catalysts did not change for the seventh and the eighth cycle. In a word, it is far not enough to mention the industrial application of these catalysts only based on the results presented and further work is in progress.

3 Conclusions

The low temperature C₃H₆-SCR has been investigated over 0.5% Pt/SBA-15 and 0.5% Pt/Al-SBA-15 catalysts. The 0.5% Pt/SBA-15 sample achieved markedly high 80.1% NO_x reduction and 87.04% C₃H₆ conversion simultaneously at 140°C. Such high catalytic activity correlates well with the outstanding oxidation activities shown in NO/C₃H₆ oxidation reactions. Higher concentrations of

O₂ and C₃H₆ led to higher NO_x conversion efficiencies. Higher Pt loading favored NO_x conversion, but an optimum content of 0.5 wt.% Pt was observed. The XPS results suggested that Pt, PtO and PtO₂ were all presented in the catalyst, whereas PtO₂ species might play a role as main active site of Pt/SBA-15. The incorporation of appropriate amount Al into SBA-15 improved catalytic performance, which could be ascribed to the enhancement of catalyst surface acidity caused by tetrahedrally coordinated AlO₄. Further studies are in progress for a deep understanding of the mechanism of low temperature C₃H₆-SCR.

Acknowledgments

This work was supported by the National Natural Science Foundation of China (No. 20807027) and the National High-Tech Research and Development Program (863) of China (No. 2010AA064907).

References

- Adamowska M, Krzton A, Najbar M, Camra J, Mariadassou G D, Costa P D, 2009. Ceria-zirconia-supported rhodium catalyst for NO_x reduction from coal combustion flue gases. *Applied Catalysis B: Environmental*, 90(3-4): 535–544.
- Beck J S, Vartuli J C, Roth W J, Leonowicz M E, Kresge C T, Schmitt K D et al., 1992. A new family of mesoporous molecular sieves prepared with liquid crystal templates. *Journal of the American Chemical Society*, 114(27): 10834–10843.
- Bera P, Hegde M S, 2011. NO reduction over noble metal ionic catalysts. *Catalysis Surveys From Asia*, 15(3): 181–199.
- Boutros M, Trichard J M, Costa P D, 2009. Silver supported mesoporous SBA-15 as potential catalysts for SCR NO_x by ethanol. *Applied Catalysis B: Environmental*, 91(3-4): 640–648.
- Brandenberger S, Kröcher O, Tissler A, Althoff R, 2008. The state of the art in selective catalytic reduction of NO_x by ammonia using metal-exchanged zeolite catalysts. *Catalysis Reviews*, 50(4): 492–531.
- Brandhorst M, Zajac J, Jones D J, Rozière J, Womes M, Jimenez-López A et al., 2005. Cobalt-, copper- and iron-containing monolithic aluminosilicate-supported preparations for selective catalytic reduction of NO with NH₃ at low temperatures. *Applied Catalysis B: Environmental*, 55(4): 267–276.
- Calleja G, Aguado J, Carrero A, Moreno J, 2007. Preparation, characterization and testing of Cr/AlSBA-15 ethylene polymerization catalysts. *Applied Catalysis A: General*, 316(1): 22–31.
- Chmielarz L, Kuśtrowski P, Dziembaj R, Cool P, Vansant E F, 2006. Catalytic performance of various mesoporous silicas modified with copper or iron oxides introduced by different ways in the selective reduction of NO by ammonia. *Applied Catalysis B: Environmental*, 62(3-4): 369–380.
- Corma A, 1997. From microporous to mesoporous molecular sieve materials and their use in catalysis. *Chemical Reviews*, 97(6): 2373–2420.
- Corro G, Fierro J G, Montiel R, Castillo S, Moran M, 2003.

- A highly sulfur resistant Pt-Sn/Al₂O₃ catalyst for C₃H₈-NO-O₂ reaction under lean conditions. *Applied Catalysis B: Environmental*, 46(2): 307–317.
- García-Cortés J M, Illán-Gómez M J, Solano A L, de Lecea C S, 2000. Low temperature selective catalytic reduction of NO_x with C₃H₆ under lean-burn conditions on activated carbon-supported platinum. *Applied Catalysis B: Environmental*, 25(1): 39–48.
- Giroir-Fendler A, Denton P, Boreave A, Praliaud H, Primet M, 2001. The role of support acidity in the selective catalytic reduction of NO by C₃H₆ under lean-burn conditions. *Topics in Catalysis*, 16-17(1-4): 237–241.
- Gorce O, Baudin F, Thomas C, Costa P D, Djéga-Mariadassou G, 2004. On the role of organic nitrogen-containing species as intermediates in the hydrocarbon-assisted SCR of NO_x. *Applied Catalysis B: Environmental*, 54(2): 69–84.
- Granger P, Parvulescu V I, 2011. Catalytic NO_x abatement systems for mobile sources: from three-way to lean burn after-treatment technologies. *Chemical Reviews*, 111(5): 3155–3207.
- Guo Y, Wang L F, Sakurai M, Kameyama H, Kudoh Y, 2006. Selective catalytic reduction of nitric oxide with propene and diesel fuel as reducing agents over anodic alumina catalyst. *Journal of Chemical Engineering of Japan*, 39(2): 162–172.
- Halkides T I, Kondarides D I, Verykios X E, 2002. Mechanistic study of the reduction of NO by C₃H₆ in the presence of oxygen over Rh/TiO₂ catalysts. *Catalysis Today*, 73(3-4): 213–221.
- Haneda M, Kintaichi Y, Bion N, Hamada H, 2003. Mechanistic study of the effect of coexisting H₂O on the selective reduction of NO with propene over sol-gel prepared In₂O₃-Al₂O₃ catalyst. *Applied Catalysis B: Environmental*, 42(1): 57–68.
- Hoost T E, Kudla R J, Collins K M, Chattha M S, 1997. Characterization of Ag/γ-Al₂O₃ catalysts and their lean-NO_x properties. *Applied Catalysis B: Environmental*, 13(1): 59–67.
- Iliopoulou E F, Evdou A P, Lemonidou A A, Vasalos I A, 2004. Ag/alumina catalysts for the selective catalytic reduction of NO_x using various reductants. *Applied Catalysis A: General*, 274(1-2): 179–189.
- Ivanova E, Mihaylov M, Thibault-Starzyk F, Daturi M, Hadjiivanov K, 2007. FTIR spectroscopy study of CO and NO adsorption and co-adsorption on Pt/TiO₂. *Journal of Molecular Catalysis A: Chemical*, 274(1-2): 179–184.
- Jang M, Park J K, Shin E W, 2004. Lanthanum functionalized highly ordered mesoporous media: implications of arsenate removal. *Microporous and Mesoporous Materials*, 75(1-2): 159–168.
- Jen H W, 1998. Study of nitric oxide reduction over silver/alumina catalysts under lean conditions: effects of reaction conditions and support. *Catalysis Today*, 42(1-2): 37–44.
- Jeon J Y, Kim H Y, Woo S I, 2003. Selective catalytic reduction of NO_x in lean-burn engine exhaust over a Pt/V/MCM-41 catalyst. *Applied Catalysis B: Environmental*, 44(4): 311–323.
- Kotsifa A, Kondarides D I, Verykios X E, 2007. Comparative study of the chemisorptive and catalytic properties of supported Pt catalysts related to the selective catalytic reduction of NO by propylene. *Applied Catalysis B: Environmental*, 72(1-2): 136–148.
- Kumar P A, Reddy M P, Ju L K, Phil H H, 2008. Novel silver loaded hydroxyapatite catalyst for the selective catalytic reduction of NO_x by propene. *Catalysis Letters*, 126(1-2): 78–83.
- Lanza R, Eriksson E, Pettersson L J, 2009. NO_x selective catalytic reduction over supported metallic catalysts. *Catalysis Today*, 147(Suppl.): S279–S284.
- Li H F, Lü J, Zheng Z L, Cao R, 2011. An efficient and reusable silica/dendrimer supported platinum catalyst for electron transfer reactions. *Journal of Colloid and Interface Science*, 353(1): 149–155.
- Li J H, Hao J M, Fu L X, Liu Z M, Cui X Y, 2004a. The activity and characterization of sol-gel Sn/Al₂O₃ catalyst for selective catalytic reduction of NO_x in the presence of oxygen. *Catalysis Today*, 90(3-4): 215–221.
- Li Y, Zhang W H, Zhang L, Yang Q H, Wei Z B, Feng Z C et al., 2004b. Direct synthesis of Al-SBA-15 mesoporous materials via hydrolysis-controlled approach. *Journal of Physical Chemistry B*, 108(28): 9739–9744.
- Liu X Y, Jiang Z, Chen M X, Zhang Z X, Shangguan W F, 2011. Low-temperature performance of Pt/TiO₂ for selective catalytic reduction of low concentration NO by C₃H₆. *Industrial & Engineering Chemistry Research*, 50(13): 7866–7873.
- Liu Z M, Woo S I, 2006. Recent advances in catalytic deNO_x science and technology. *Catalysis Reviews*, 48(1): 43–89.
- Luo Y M, Hao J M, Hou Z Y, Fu L X, Li R T, Ning P et al., 2004. Influence of preparation methods on selective catalytic reduction of nitric oxides by propene over silver-alumina catalyst. *Catalysis Today*, 93-95(S1): 797–803.
- Matyshak V A, Sadykov V A, Chernyshov K A, Ross J, 2009. *In situ* FTIR study of the formation and consumption routes of nitroorganic complexes-intermediates in selective catalytic reduction of nitrogen oxides by propene over zirconia-based catalysts. *Catalysis Today*, 145(1-2): 152–162.
- Nguyen L Q, Salima C, Hinode H, 2010. Roles of nano-sized Au in the reduction of NO_x by propene over Au/TiO₂: An *in situ* DRIFTS study. *Applied Catalysis B: Environmental*, 96(3-4): 299–306.
- Patel A, Rufford T E, Rudolph V, Zhu Z H, 2011. Selective catalytic reduction of NO by CO over CuO supported on SBA-15: Effect of CuO loading on the activity of catalysts. *Catalysis Today*, 166(1): 188–193.
- Pitchon V, Fritz A, 1999. The relation between surface state and reactivity in the deNO_x mechanism on Platinum-based catalysts. *Journal of Catalysis*, 186(1): 64–74.
- Ravikovitch P I, Neimark A V, 2001. Characterization of micro- and mesoporosity in SBA-15 materials from adsorption data by the NLDFT method. *Journal of Physical Chemistry B*, 105(29): 6817–6823.
- Rico M J O, Moreno-Tost R, Jiménez-López A, Rodríguez-Castellón E, Pere-níguez R, Caballero A et al., 2010. Study of nanoporous catalysts in the selective catalytic reduction of NO_x. *Catalysis Today*, 158(1-2): 78–88.
- Roy S, Hegede M S, Madras G, 2009. Catalysis for NO_x abatement. *Applied Energy*, 86(11): 2283–2297.
- Salem I, Courtois X, Corbos E C, Marecot P, Duprez D, 2008. NO

- conversion in presence of O₂, H₂O and SO₂: improvement of a Pt/Al₂O₃ catalyst by Zr and Sn, and influence of the reducer C₃H₆ or C₃H₈. *Catalysis Communications*, 9(5): 664–669.
- Sayari A, 1996. Catalysis by crystalline mesoporous molecular sieves. *Chemistry of Materials*, 8(8): 1840–1852.
- Segura Y, Chmielarz L, Kustrowski P, Cool P, Dziembaj R, Vansant E F, 2005. Characterisation and reactivity of vanadia-titania supported SBA-15 in the SCR of NO with ammonia. *Applied Catalysis B: Environmental*, 61(1-2): 69–78.
- Seker E, Gulari E, 2000. Activity and N₂ selectivity of sol-gel prepared Pt/alumina catalysts for selective NO_x reduction. *Journal of Catalysis*, 194(1): 4–13.
- Sumiya S, Oumi Y, Uozumi T, Sano T, 2001. Characterization of AISBA-15 prepared by post-synthesis alumination with trimethylaluminium. *Journal of Materials Chemistry*, 11(4): 1111–1115.
- Wang X P, Xu Y, Yu S S, Wang C, 2005. The first study of SCR of NO_x by acetylene in excess oxygen. *Catalysis Letters*, 103(1-2): 101–108.
- Yentekakis I V, Tellou V, Botzolaki G, Rapakousios I A, 2005. A comparative study of the C₃H₆ + NO + O₂, C₃H₆ + O₂ and NO + O₂ reactions in excess oxygen over Na-modified Pt/γ-Al₂O₃ catalysts. *Applied Catalysis B: Environmental*, 56(3): 229–239.
- Yue Y H, Gédéon A, Bonardet J L, D'Espinose J B, Fraissard J, Melosh N, 1999. Direct synthesis of AISBA mesoporous molecular sieves: characterization and catalytic activities. *Chemical Communications*, (19): 1967–1968.
- Zhao D Y, Feng J L, Huo Q S, Melosh N, Fredrickson G H, Chmelka B F et al., 1998. Triblock copolymer syntheses of mesoporous silica with periodic 50 to 300 angstrom pores. *Science*, 279(5350): 548–552.

JOURNAL OF ENVIRONMENTAL SCIENCES

环境科学学报(英文版)
(<http://www.jesc.ac.cn>)

Aims and scope

Journal of Environmental Sciences is an international academic journal supervised by Research Center for Eco-Environmental Sciences, Chinese Academy of Sciences. The journal publishes original, peer-reviewed innovative research and valuable findings in environmental sciences. The types of articles published are research article, critical review, rapid communications, and special issues.

The scope of the journal embraces the treatment processes for natural groundwater, municipal, agricultural and industrial water and wastewaters; physical and chemical methods for limitation of pollutants emission into the atmospheric environment; chemical and biological and phytoremediation of contaminated soil; fate and transport of pollutants in environments; toxicological effects of terrorist chemical release on the natural environment and human health; development of environmental catalysts and materials.

For subscription to electronic edition

Elsevier is responsible for subscription of the journal. Please subscribe to the journal via <http://www.elsevier.com/locate/jes>.

For subscription to print edition

China: Please contact the customer service, Science Press, 16 Donghuangchenggen North Street, Beijing 100717, China. Tel: +86-10-64017032; E-mail: journal@mail.sciencep.com, or the local post office throughout China (domestic postcode: 2-580).

Outside China: Please order the journal from the Elsevier Customer Service Department at the Regional Sales Office nearest you.

Submission declaration

Submission of an article implies that the work described has not been published previously (except in the form of an abstract or as part of a published lecture or academic thesis), that it is not under consideration for publication elsewhere. The submission should be approved by all authors and tacitly or explicitly by the responsible authorities where the work was carried out. If the manuscript accepted, it will not be published elsewhere in the same form, in English or in any other language, including electronically without the written consent of the copyright-holder.

Submission declaration

Submission of the work described has not been published previously (except in the form of an abstract or as part of a published lecture or academic thesis), that it is not under consideration for publication elsewhere. The publication should be approved by all authors and tacitly or explicitly by the responsible authorities where the work was carried out. If the manuscript accepted, it will not be published elsewhere in the same form, in English or in any other language, including electronically without the written consent of the copyright-holder.

Editorial

Authors should submit manuscript online at <http://www.jesc.ac.cn>. In case of queries, please contact editorial office, Tel: +86-10-62920553, E-mail: jesc@263.net, jesc@rcees.ac.cn. Instruction to authors is available at <http://www.jesc.ac.cn>.

Journal of Environmental Sciences (Established in 1989)

Vol. 25 No. 5 2013

Supervised by	Chinese Academy of Sciences	Published by	Science Press, Beijing, China
Sponsored by	Research Center for Eco-Environmental Sciences, Chinese Academy of Sciences		Elsevier Limited, The Netherlands
Edited by	Editorial Office of Journal of Environmental Sciences P. O. Box 2871, Beijing 100085, China Tel: 86-10-62920553; http://www.jesc.ac.cn E-mail: jesc@263.net , jesc@rcees.ac.cn	Distributed by	
		Domestic	Science Press, 16 Donghuangchenggen North Street, Beijing 100717, China Local Post Offices through China
		Foreign	Elsevier Limited http://www.elsevier.com/locate/jes
Editor-in-chief	Hongxiao Tang	Printed by	Beijing Beilin Printing House, 100083, China
CN 11-2629/X	Domestic postcode: 2-580		Domestic price per issue RMB ¥ 110.00

ISSN 1001-0742



9 771001 074130